Environmental Technology & Innovation 36 (2024) 103867

Contents lists available at ScienceDirect

Environmental Technology & Innovation

journal homepage: www.elsevier.com/locate/eti

# Biodegradation of tri-butyl phosphate by *Trametes versicolor* and its application in a trickle bed reactor under non-sterile conditions

Shamim Tayar [a], Diana Losantos [a], Javier Villagra [d], Kaidi Hu [b], Soheila Shokrollahzadeh [c], Montserrat Sarrà [a,*], Núria Gaju [d], Maira Martínez-Alonso [d]

[a] *Departament d'Enginyeria Química Biològica i Ambiental, Escola d'Enginyeria, Universitat Autònoma de Barcelona, Bellaterra, Barcelona 08193, Spain*
[b] *College of Food Science, Sichuan Agricultural University, Ya'an, Sichuan 625014, People's Republic of China*
[c] *Department of Chemical Technologies, Iranian Research Organization for Science and Technology (IROST), Tehran, Iran*
[d] *Departament de Genètica i Microbiologia, Universitat Autònoma de Barcelona, Bellaterra, Barcelona 08193, Spain*

ARTICLE INFO

*Keywords:*
Emerging pollutant
Flame retardants
Fungal treatment
Laccase
Microbial assemblage

ABSTRACT

Tri-butyl phosphate (TBP) is a widely used organophosphate flame retardant. However, it is also regarded as emerging contaminant due to its various toxic effects and poor removal by conventional wastewater treatment. In present study, we investigated the degradation of TBP (10 mg/L) by the white rot fungus *Trametes versicolor* in both laboratory conditions and a trickle bed reactor (TBR) under non-sterile conditions. The removal yield reached 98 % after 3 days, during which the intracellular enzymatic system cytochrome P450 was involved. Four transformation products (TPs) were identified, namely dibutyl 3-hydroxybutyl phosphate, dibutyl phosphate, butyl 3-hydroxybutyl phosphate and butyl dihydrogen phosphate, which allowed us to propose a degradation pathway where hydroxylation and hydrolysis made considerable contribution. TBP treatment in the TBR with *T. versicolor* immobilized on wood chips operating in sequential batch mode with 10 cycles of 3 days reached average removals higher than 93 %, demonstrating the potential for practical application. Despite similar removal rates in heat-killed and abiotic controls (89 % and 97 %, respectively), global mass balance analysis indicated 86 %, 64 %, and 86 % removal by degradation in the fungal, heat-killed, and abiotic controls, respectively. Analysis of the microbial assemblage in solid phase suggested that the established bacterial populations displayed a synergistic effect with immobilized fungus. This study is the first to report on TBP degradation by *T. versicolor* in a TBR under non-sterile conditions, suggesting that this method could be a viable option for large-scale environmental applications.

## 1. Introduction

Organophosphate flame retardants (OPFRs) are alkyl esters of phosphoric acid that are used as additives in a variety of commercial products including plastics, foams, paints, textiles, and furniture due to their physicochemical characteristics, which allows them to act as flame retardant barriers (Martínez-Carballo et al., 2007). OPFRs are not chemically bonded to their host materials, and therefore can

* Corresponding author.
*E-mail address:* Montserrat.Sarra@uab.cat (M. Sarrà).

https://doi.org/10.1016/j.eti.2024.103867
Received 23 August 2024; Received in revised form 30 September 2024; Accepted 19 October 2024
Available online 22 October 2024

easily diffuse by volatilization, leaching, or abrasion processes into surrounding environments, especially in water compartments (Reemtsma et al., 2008). Considering that many OPFRs have been demonstrated to be toxic directly linked to health problems and persistent in the environment, they are now considered emerging pollutants (Wolschke et al., 2015). Tributyl phosphate (TBP) is a major member of OPFRs. Likewise, several toxic effects of TBP have been reported in rats and mice (Arnold et al., 1997; Auletta et al., 1998). TBP can also inhibit the growth of unicellular algae, protozoa, and bacteria and be toxic to fish (World Health Organization, 1991). On the other hand, TBP causes skin, eyes, and mucous membranes irritations at small concentrations, and can be neurotoxic for humans (Kulkarni et al., 2014).

TBP is only partially removed in wastewater treatment plants (WWTPs), as it has been reported as one of the prevailing compounds WWTPs effluents (Marklund et al., 2005; Martínez-Carballo et al., 2007; Meyer and Bester, 2004; Rodil et al., 2012; Shi et al., 2016). In this matter, there is an important exposure pathway for TBP to humans, as this compound has not only been reported in fish specimens (Kim et al., 2011; Santín et al., 2016), but also in tap water samples (Bacaloni et al., 2007; Rodil et al., 2012), proving once again that conventional treatment facilities are not enough for its elimination.

New physicochemical eliminating methods have been developed in recent years to address such concern, including ozonation (Pocostales et al., 2010; Yuan et al., 2015), UV/$H_2O_2$ treatments (Yuan et al., 2015), Fenton-based reactions (Watts and Linden, 2008; Yang et al., 2022) and gliding arc plasma (Moussa and Brisset, 2003). However, these approaches can be expensive, produce toxic compounds, and emit heat (Kulkarni et al., 2014). For these reasons, bioremediation progressively appears as an appealing alternative as it is simple, efficient, and economically feasible (Kulkarni et al., 2014).

Many microbial groups have detoxifying abilities (i.e. mineralization, transformation, and/or immobilization of pollutants), and these biological methods have been considered environmentally friendly (Dang et al., 2023). Bioremediation treatments of wastewater are usually performed by bacteria because of their catabolic capacities. However, fungi, specifically white rot fungi (WRF), can constitutively, and co-metabolically degrade a series of contaminants that are present at trace concentrations. This intrinsic ability comes from the fact that they efficiently break down lignin through extracellular ligninolytic enzymes (laccase, lignin peroxidase, manganese peroxidase, and versatile peroxidase) that are non-specific. Furthermore, WRF possess a versatile intracellular system called cytochrome P450, which plays a role in maintaining biochemical reactions but is also responsible for contaminants fungal degradation in many cases (Mir-Tutusaus et al., 2018). However, one of the key challenges in applying WRF in real-world wastewater treatment is their competition with indigenous microorganisms, especially under non-sterile conditions.

To address this, our previous research demonstrated the efficacy of *T. versicolor* in degrading TBP and other OPFRs under controlled conditions. For instance, we established the importance of maintaining aerobic conditions for optimal fungal activity, with oxygen levels significantly impacting degradation efficiency and enzyme production (Beltrán-Flores et al., 2023). Additionally, our studies identified the enzymatic pathways involved in OPFR degradation and highlighted the potential of *T. versicolor* in co-culture systems for enhanced pollutant removal (Losantos et al., 2024).

Building on these foundational studies, the current research focuses on applying *T. versicolor* in a trickle bed reactor (TBR) under non-sterile conditions. TBRs are advantageous for wastewater treatment due to their high surface area for colonization, efficient substrate contact, and scalability for industrial applications (Feickert Fenske et al., 2023; Hu et al., 2021). By immobilizing *T. versicolor* on oak wood chips, the TBR provides a supportive environment that enhances fungal stability and pollutant degradation efficiency (Hu et al., 2022).

This study evaluates the performance of *T. versicolor* in a non-sterile TBR, assessing its ability to degrade TBP over multiple cycles. The research mimics real-world scenarios, emphasizing the importance of testing proven fungal degradation capabilities in practical, non-sterile environments. By investigating the interactions between fungal and bacterial populations within the TBR, we aim to provide comprehensive insights into the microbial dynamics that drive effective bioremediation.

To the best of our knowledge, this is the first work reporting TBP degradation by *T. versicolor* in a trickle bed reactor under non-sterile conditions in sequencing batch mode. Microbial diversity and relative abundance of prominent fungal and bacterial populations on woodchips were carried out by combining PCR_DGGE and sequencing. Moreover, *T. versicolor*, total fungal and bacterial abundances were estimated by using qPCR. This innovative approach not only confirms the degradation pathways involving cytochrome P450 and laccase enzymes but also explores the synergistic effects between fungi and bacteria, setting the stage for future developments in bioremediation technologies aimed at addressing persistent organic pollutants.

## 2. Materials and methods

### 2.1. Microorganisms and media

*Trametes versicolor* ATCC 42530 was acquired from American Type Culture Collection and maintained by subculturing every 30 days on malt extract agar (pH 4.5) at 25 ºC. Blended mycelial suspensions and pellets were prepared following the methods described by Blánquez et al. (Blánquez et al., 2004). Packing material for trickle bed reactor was prepared by inoculating mycelial suspension on oak wood chips (sieve mesh sizes between 7.10 and 16 mm) as described by Hu et al. and then keep at 25 °C for 50 days (Hu et al., 2022).

Defined medium was utilized for batch degradation experiments, which was composed of 8 g/L glucose, 3.3 g/L ammonium tartrate, 1.68 g/L dimethyl succinate, 10 mL/L micronutrients and 100 mL/L macronutrient (Kirk et al., 1978). pH was adjusted to 4.5 prior to autoclave at 121 °C for 15 min.

### 2.2. Chemicals and reagents

Tributyl phosphate of analytical grade (purity, > 99 %), commercial laccase purified from *T. versicolor* (20 AU/mg), laccase mediator 2,2'-azino-bis (3-ethylbenzothriazoline-6-sulphonic acid) diammonium salt (ABTS, 98 %), 2,6-dymetoxyphenol (DMP, 99 %), cytochrome P450 (CYP450) inhibitor 1-aminobenzotriazole (ABT) (98 %) were purchased from Sigma-Aldrich (Barcelona, Spain). Chromatographic grade methanol, acetonitrile and formic acid ($\geq$ 98 %) used as a mobile phase modifier were obtained from Merck (Darmstadt, Germany). Microtox bioassay kit was supplied by Strategic Diagnostics (Newark, USA). All other chemicals used were of analytical grade and acquired from Sigma-Aldrich (Barcelona, Spain).

### 2.3. Degradation of TBP by T. versicolor in Erlenmeyer flasks

Degradation experiments were performed in 250 mL Erlenmeyer flasks containing 50 mL of defined medium fortified with TBP at a final concentration of 10 mg/L. Fungal pellets were transferred into flasks as inoculum, thereby achieving a concentration of approximately 3.5 g dry weight (DW)/L. Then the cultures were incubated at 25 °C under continuous orbital-shaking (135 rpm) for 7 days. To obviate the influence of photodegradation, incubation was performed in the dark. Abiotic (uninoculated) and heat-killed culture (121 °C for 30 min) were used as controls. Triplicates were running for each set and samples were withdrawn at designed intervals to determine TBP and glucose concentrations.

### 2.4. Evaluation of the enzymatic system involved in TBP degradation by T. versicolor

To investigate the role of different enzymatic systems during TBP decomposition by *T. versicolor*, *in vitro* and *in vivo* degradation experiments were carried out. Specifically, laccase-mediated degradation experiments were conducted in 250 mL Erlenmeyer flasks containing 50 mL laccase-sodium malonate dibasic monohydrate solution (250 mM, pH 4.5) at a final enzyme activity of 1000 AU/L, in which TBP was spiked up to 10 mg/L. The effect of laccase mediator ABTS (0.8 mM) on substrate degradation was evaluated by comparing with the results of culture where the mediator was not present (Marco-Urrea et al., 2009). Abiotic control (no laccase) was run simultaneously, and all sets were prepared in triplicate. The flasks were kept for 48 h on an orbital shaker (135 rpm) at 25 °C. At designated times, one mL aliquots were collected and mixed with 100 μL of 1 M HCl to stop the reaction, followed by filtrating through a Millipore Millex-GV unit equipped with polyvinylidene difluoride (PVDF) membrane (0.22 μm) before TBP quantification. With respect to CYP450, ABT was fortified into aforementioned pellets-TBP incubation system, to a final concentration of 5 mM (Marco-Urrea et al., 2009). The initial biomass and TBP concentration were 3.5 g DW/L and 10 mg/L, respectively. An inhibitor-free control was also set, and all the cultures were incubated at 25 °C in the dark for 7 days under shaken condition (135 rpm). Each group consisted of three repetitions. Samples were collected at designated times to measure TBP concentration.

### 2.5. Identification of tributyl phosphate transformation products

Degradation experiments were carried out as described previously (Section 2.3) with 500 mL Erlenmeyer flasks containing 100 mL of fresh defined medium. After 7 days incubation, each flask was totally sacrificed, and the culture was firstly filtrated through a Whatman™ glass microfiber filter (GF/A, 47 mm). Then, 20 mL of obtained filtrates were mixed with 50 μL of internal standard (IS), followed by adding filtrates up to 50 mL. Both liquid and solid (biomass) samples were kept at – 20 °C until analysis.

### 2.6. Tributyl phosphate removal in trickle bed reactor under non-sterile condition

A lab-scale trickle bed reactor (TBR) essentially consisted of a vertical cylindrical fixed bed, a liquid recirculation system and pH maintenance as previously described (García-Vara et al., 2021). After incubation, the fungal colonized wood chips were transferred into a methacrylate tube (Ø 8.5 cm, H 58 cm) and supported by a mesh, achieving an approximate working volume of 2.5 L and a porosity of 60 %. The synthetic wastewater (SWW), composed of 100 mL/L macronutrient, 10 mL of micronutrient and 10 mg/L of TBP, was loaded into the packing bed from the top of reactor through a rotary distributor and then collected by the reservoir tank placed at the bottom. The collected water was mixed by a magnetic stirrer, and its pH was maintained at 4.5 by adding either 1 M HCl or 1 M NaOH. An external bottom-to-top recirculation loop (70 mL/min) was provided, by which the collected water was continuously fed into the packing bed. Simultaneously, another two identical reactors filled with heat killed colonized wood (killed control, KC) and non-colonized chips (abiotic control, AC) were operated in parallel, to assess the adsorption from the biomass and lignocellulosic supporting material, respectively. Multiple runs were implemented in sequencing batch mode at room temperature, and a 3-day cycle was fixed. Samples were taken from the tank after each batch to measure TBP concentration, turbidity and chemical oxygen demand (COD). Then, the SWW was totally replenished.

### 2.7. Microbial community analysis

#### 2.7.1. Immobilized biomass extraction

To extract the microbial biomass from woodchips, a sterile phosphate buffer consisting of $KH_2PO_4$ 5.3 g/L and $K_2HPO_4$ 10.6 g/L in ultra-pure and sterile filtered water solution was used. The woodchips were submerged in 50 mL of buffer solution inside sterile bags, agitated at 200 rpm for 30 min, and sonicated in a Selecta ultrasound bath for 7 min at 40 kHz. The biomass suspension was then

centrifuged at 8500 rpm and, the pellets were weighted and preserved at −20 ºC. Dry mass from woodchips was determined by heating at 60 ºC until weight stabilization.

#### 2.7.2. Total DNA extraction and DNA amplification

DNA was extracted by using a DNA DNeasy® PowerSoil® Pro Kit from Qiagen, following manufacturer's instructions. The extracts were quantified using a Qubit 3.0 fluorometer together with the dsDNA High Sensitivity assay Kit from Thermo Fisher Scientific. DNA extractions for each condition were performed by triplicate. DNA was subsequently amplified as detailed in the supplementary material using the primers and PCR conditions described in Table S1.

#### 2.7.3. DGGE Fingerprinting analysis

DGGE in a 6 % (w/v) acrylamide gel was performed to obtain the fingerprint of fungal and bacterial community for each condition, including the initial stage of colonized wood. For the fungal amplicons, the chemical denaturing gradient of the gel was from 15 % to 55 %, while it varied from 30 % to 70 % in the case of bacterial PCR products. Gradients were formed with 6 % (w/v) acrylamide stock solutions (acrylamide-N:N′-methylene-bis-acrylamide, 37.5:1) where the 100 % denaturing solution contained 7 M urea (Bio-Rad) and 40 % (v/v) formamide (Merck) deionized with AG501-X8 mixed-bed resin (Bio-Rad). 1200 ng of each sample were loaded on the gel and run in TAE 1X buffer (40 mM Tris acetate at pH 7.4, 20 mM sodium acetate, 1 mM EDTA), with a stacking run of 20 min at 10 V and a migration run of 16 h at 75 V. The electrophoresis was performed with the Dcode Universal Mutation Detection System (Bio-Rad). The gel was then stained with ethidium bromide (0.5 mg/L) and photographed in a Bio-Rad Gel Doc system.

#### 2.7.4. Sequencing

Prominent bands were excised and placed in Eppendorf tubes containing 50 µL of 1X PCR Rxn buffer and stored at 4ºC for 24 hours to allow DNA diffusion before re-amplification. Amplified DGGE bands recovered from the gel were sequenced by Macrogen, Inc. (South Korea). Sequences were manually trimmed, and quality checked using FinchTV 1.4.0 (Geospizza, Inc.). Curated sequences were deposited in the National Center for Biotechnology Information (NCBI) GenBank database under accession numbers OR327567 to OR327602 for Bacteria and OR352313 to OR352358 for Fungi.

#### 2.7.5. Quantitative real-time PCR (qPCR)

qPCR of total bacteria, total fungi and specifically for *Trametes versicolor* were carried out with the primer sets Com1 (5'-CAGCAGCCGCGGTAATAC-3')/769 R (5'-ATCCTGTTTGMTMCCCVCRC-3'), ITS3 (5'-GCATCGATGAAGAACGCAGC-3')/ITS4 (5'-TCCTCCGCTTATTGATATGC-3') and TvQF (5'-CACGCTCTGCTCATCCACTCT-3')/TvQR (5'- GCAGAATGCTCCCGTTAAGG −3'), respectively. qPCR assays were performed in a Bio-Rad CFX96™ Real-Time System C1000™ Thermal Cycler controlled by Bio-Rad CFX Manager software using the cycling conditions described by Dorn-In et al. (Dorn-In et al., 2015), Maza-Márquez et al., (Maza-Márquez et al., 2018) and Eikenes et al., (Eikenes et al., 2005) respectively. Each reaction mixture, with a final volume of 20 µL, contained 1× ssoAdvanced Universal SYBR Green Supermix (Bio-Rad), 1 µM, 0.5 µM and 0.3 µM of each forward and reverse primers for total bacteria, total fungi and *Trametes versicolor*, respectively, and 36 ng of DNA template. All reactions were run by triplicate with a resulting amplification efficiency of 116.62 % and $r^2$ value of 0.989 for bacteria, 105.51 % and $r^2$ value of 0.995 for fungi and 118.17 % and $r^2$ value of 0.996 for *Trametes versicolor*. Calibration curves were prepared with known amounts of *Salmonella* sp. (CT =−2.9979*log(conc) + 25.877), *Trichoderma harzianum* (CT=-3.197*log(conc) +28.809), *T. versicolor* ATCC 42530 (CT=-2.952*log (conc) +30.554).

### 2.8. Analytical methods

#### 2.8.1. Biomass quantification

Biomass in terms of pellets was determined by the dry weight, obtained after filtrating the culture and drying the residue at 105 °C to a constant weight.

#### 2.8.2. Laccase activity

After filtrating by 0.22 µm hydrophilic polypropylene syringe filter (Scharlau, Barcelona, Spain), laccase activity was measured through the oxidation of DMP by the enzyme as described elsewhere (Wariishi et al., 1992). Activity units per liter (AU/L) are defined as the amount of DMP in µM, which is oxidized in one minute. The molar extinction coefficient of DMP was 24.8/(mM cm).

#### 2.8.3. Tributyl phosphate concentration

TBP chromatography study was adapted from a method previously described elsewhere (Kraft et al., 2015). This analysis was performed using a Prominence UFLC that was controlled by an LCMSsolution Chromatography Data System software, consisting of a SIL/20 A autosampler and LC-20AD solvent-delivery system and equipped with a LCMS-2010A detector, all of them from Shimadzu (Japan). Chromatographic separation was achieved by an Acclaim Organic Acid (OA) column from Dionex, OA 5 µm, 120 Å, 4.0 × 150 mm (Thermo Scientific, Waltham, USA). The column temperature was 30 ºC. The mobile phase consisted of 75 % methanol and 25 % ultrapure water (v/v), which was pumped isocratically at 0.25 mL/min. The injection volume was 2 µL. The mass spectrometer was operated in the selected ion monitoring (SIM), electrospray ionization, positive mode (ESI+) and was set up to monitor the ions *m/z* 267.10. Data in the tuning file were selected for parameters such as lens voltage values, Interface, Q-array and others. High purity nitrogen was used as nebulizing gas at 1.50 L/min and drying gas pressure was 0. The detection voltage was set at 1.5 kV. The other

operation parameters for MS were optimized as follows: capillary voltage 4.50 kV; heat block temperature, 200 °C; CDL temperature, 250 °C.

*2.8.4. Evaluation and identification of transformation products*

Identification of TPs was performed on an ultra-high performance liquid chromatograph equipped with a hybrid quadrupole-Orbitrap mass spectrometer (UHPLC-Q-Exactive, Thermo Fisher Scientific). Chromatographic separation was carried out on a Purospher® STAR RP-18 endacapped Hibar® HR (150 × 2.1 mm, 2 μm) UHPL column (Merck, Germany). Acetonitrile and ultrapure water containing 0.1 % (v/v) formic acid plus 5 mM ammonium acetate were used as mobile phases A and B, respectively. A gradient elution program was started with 20 % (v/v) A from 0 min to 1 min, increasing to 95 % at 8 min and held until 13 min. Then the percentage of A was further reverted to 20 % by 13.5 min and maintained it until 15 min. The follow rate was 0.2 mL/min with an injection volume of 10 μL.

The MS harbors an electrospray ionization (ESI) source, for which the specific conditions adopted were: capillary voltage, 3000 V; sheath gas, 40 arbitrary units; auxiliary gas, 10 arbitrary units; capillary temperature, 350 °C and vaporizer temperature, 300 °C. The mass spectrometer performed a Fourier Transform Mass Spectrometry (FTMS) scan event of 50–700 *m/z* at a resolution of 70, 000 and a subsequent MS/MS scan event acquired at a resolution of 35, 000. The obtained data was processed using Compound Discoverer and Xcalibur software (Thermo Fisher Scientific). Potential TPs were identified based on molecular formula, mass accuracy and degree of unsaturation of the parent ion and product ions.

*2.8.5. Other analyses*

Glucose concentration was measured using a biochemistry analyzer (2700 select, Yellow Springs Instrument, USA) after filtrating the sample with a Millipore Millex-GV PVDF syringe filter (0.22 μm). The absorbance at a wavelength of 650 nm was determined by a UNICAM 8625 UV/VIS spectrometer. The COD was analyzed by using the commercial kits LCK 314 or LCK 114 or LCK 514 (Hach Lange, Germany).

## 2.9. Data processing and Statistical analysis

Fingerprinting profiles of DGGE described in Section 2.7.5 were processed using InfoQuest™ FP version 4.5 generating an intensity matrix that was further handled by clustering analysis on a Dice distance matrix including sequenced and non-sequenced bands, in addition relative abundance of each taxonomical group, as well as Shannon's diversity index (H) (Shannon, 1984) and Pielou's evenness index (E) (Pielou, 1966) were calculated from the intensity matrix. Finally, phylotype richness (R) for each genetic profile was calculated as the mean number of bands.

The mean and standard deviation (SD) of data were calculated and subjected to statistical significance determination using SPASS v22.0 and GraphPad Prism 8.

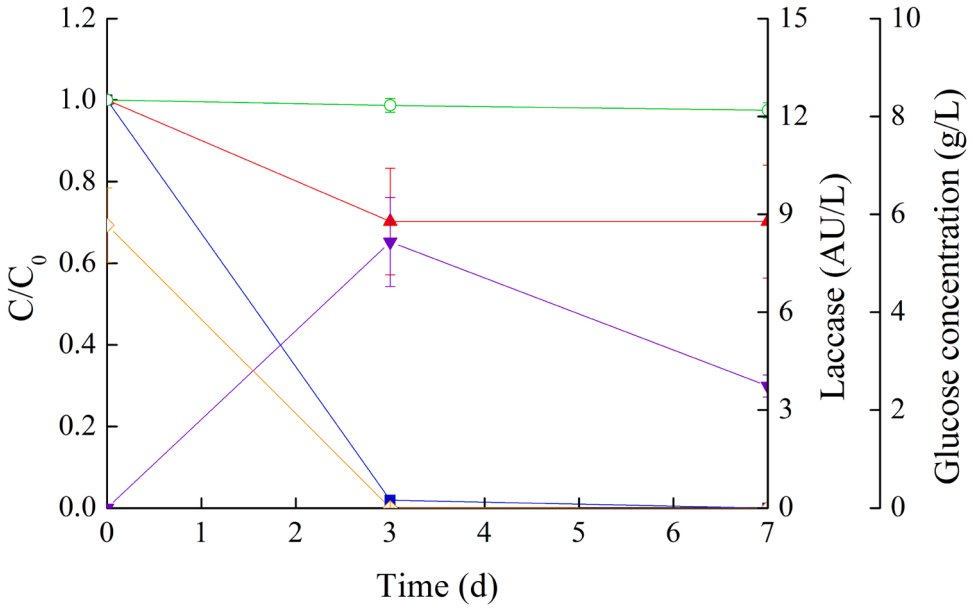


**Fig. 1.** Time-course of TBP removal by *T. versicolor*. C represents the residual concentration of TBP in the sample (mg/L), and $C_0$ corresponds to the initial concentration of TBP in the sample (mg/L). *Filled squares (colored in blue)*, experimental; *filled triangles (colored in red)*, killed control; *empty circles (colored in green)*, abiotic control; *inverted filled triangles (colored in purple)*, laccase activity; *empty rhombus (colored in orange)*, glucose concentration. Average values of three replicates with the corresponding standard deviations are shown.

qPCR results for *T.versicolor* from experimental and control reactors and *T.versicolor* with total fungi from initial colonization wood were compared for significant differences with a Kolmogorov-Smirnov test since means did not fit a normal distribution. Total fungal abundances were compared with a Kruskal-Wallis test since values didn't follow a normal distribution either, or Dum's test was used to determine which groups were significantly different. Finally, total bacterial abundances were compared with a Brown-Forsythe and Welch's ANOVA tests since residuals followed Gaussian distribution, but equal variances could not be assumed, and, in this case, Games-Howell's multiple comparisons test was used to determine where significant differences lay.

## 3. Results and discussion

### 3.1. Degradation of tributyl phosphate by T. versicolor

The ability of *T. versicolor* in degrading TBP was initially examined. As it depicted in Fig. 1, almost complete elimination was achieved after 3 d, in which the contribution from adsorption was around 20 % according to the TBP removal profile in killed control experiments. The fortified pollutant demonstrated chemical stability in abiotic control conditions. In fact, the adsorption is governed by physical-chemical characteristics of targeted compounds and adsorbent, where different yields have been obtained using *T. versicolor* (García-Vara et al., 2021; Hu et al., 2020; Lucas et al., 2018). A maximum laccase activity (8.46 AU/L) was reached on the 3rd incubation day and then declined. The variation of glucose concentration synchronized with the degradation profile, since it plunged to almost zero after 3 d.

Results from batch degradation experiments indicated that adsorption from biomass significantly contributed to total removal. To understand the fate of adsorbate, global mass balances were conducted targeting the whole cultivation system prior to TPs identification. As presented in Table 1, the TBP residues in solid and liquid phase accounted for less than 0.1 % of introduced amount, which means substantial removal (> 99 %) in the experimental treatment must be exclusively attributed to biodegradation mechanism. But adsorption can be considered as the first step during fungal elimination. A similar phenomenon has been reported by Hu et al. (Hu et al., 2020).

### 3.2. Role of laccase and cytochrome P450 enzymatic system in the degradation of TBP by T. versicolor

As aforementioned, certain laccase activity was detected during incubation. Thus, several *in vitro* experiments were carried out to confirm whether laccase and laccase-mediator systems are involved in TBP degradation. Results showed that more than 87 % of spiked TBP was removed in the presence of laccase mediator. On the contrary, although laccase activity maintained at around 45 AU/L, the degradation rate was less than 10 % in the absence of ABTS (Fig. 2a). Similar behavior was found by Mir-Tutusas et al. when working with imiprothrin (Mir-Tutusaus et al., 2014). Laccase with the mediator ABTS can oxidize non-phenolic compounds via an electron transfer route (Baiocco et al., 2003). It is also worthy to mention that there is no TBP removal using fungal broth (pellets-free 3 d-culture medium) after 24 h treatment, probably ascribed to the natural mediators secreted by fungus failed to promote the oxidation of TBP.

Aside from laccase, the contribution of CYP450 system to TBP removal was assessed through *in vivo* degradation experiments. Obviously, the degradation rate was considerably slowed down by the addition of CYP450 inhibitor ABT, compared to inhibitor-free group (Fig. 2b). The final removal in inhibited and inhibitor-free flasks were 25 % and 95 %, respectively. This observation is indicative of the indispensable contribution of CYP450 to the substrate depletion.

### 3.3. Transformation products generated during the TBP degradation by T. versicolor

Regarding TPs, a total of four compounds were captured and identified within 7 d incubation according to the results of UHPLC-MS/MS analysis. They are dibutyl 3-hydroxybutyl phosphate (OH-TBP), dibutyl phosphate (DBP), butyl 3-hydroxybutyl phosphate (OH-DBP) and butyl dihydrogen phosphate (MBP), together with their chromatographic characteristics summarized in Table S2. Given the obtained formulae, it is speculated that hydroxylation possibly occurred in the first place to generate OH-TBP. As a matter of fact, hydroxylation mediated by CYP450 is generally the first detoxification step in eukaryotes and mammals towards a wide range of contaminants, through which their hydrophilicity and bioaccessibility are enhanced (Črešnar and Petrič, 2011). CYP450 monooxygenases are generally the enzymes responsible for this first step (Eltoukhy et al., 2022). This matches well with our finding that CYP450 is considerably involved in TBP degradation (Section 3.2). Subsequently, OH-TBP underwent twice hydrolysis, yielding MBP. Simultaneously, TBP could be metabolized to MBP directly through a stepwise cleavage of the ester bonds, keeping in line with previous studies (Liu et al., 2019; Nancharaiah et al., 2015). The cleavage of ester linkage is mostly catalyzed by phosphoesterases

**Table 1**
Mass balance profile of TBP in Erlenmeyer flasks after 7 d incubation.

| Item | Mass (ng) |
|---|---|
| Introduced | 657634.92 |
| Remained in solid phase | 311.98 ± 34.90 |
| Remained in liquid phase | 521.01 ± 360.53 |
| Degradation | 656801.92 |

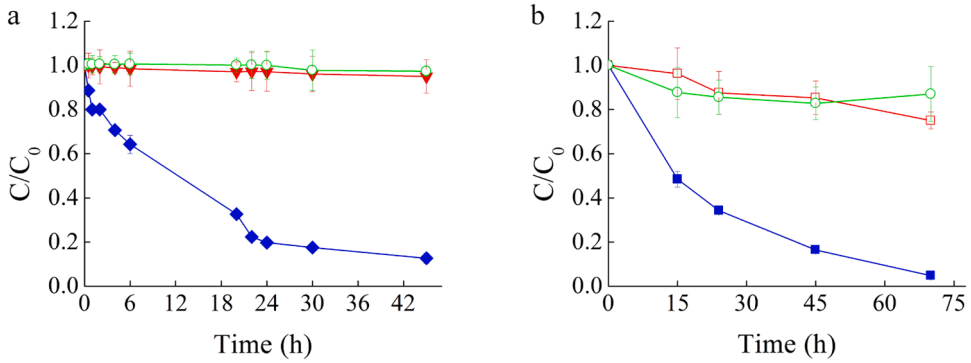


**Fig. 2.** Contribution of laccase and CYP450 system in TBP degradation. a. Degradation profile of TBP in laccase-ABTS system; b. Degradation profile of TBP by *T. versicolor* in the presence and absence of ABT inhibitor. *Filled rhombus (colored in blue)*, laccase-ABTS; *inverted filled triangles (colored in red)*, laccase; *empty circles (colored in green)*, abiotic; *filled squares (colored in blue)*, inhibitor-free; *empty squares (colored in red)*, in the presence of inhibitor. Average values of three replicates with the corresponding standard deviations are shown.

(Nancharaiah et al., 2015), which are crucial in microbial degradation of other OPFRs, such as triisobutyl phosphate (Yao et al., 2023). Phosphatases might also be involved, as high specific activity for MBP hydrolysis has been reported during microbial degradation of TBP (Rangu et al., 2022). It is likely in this case, the hydroxylation was available to took place on one butyl side chain of DBP. To our best knowledge, hydroxy-TBP has been identified as microbial degradation by-product of TBP (Hou et al., 2021), however, the formation of hydroxy-DBP was reported for the first time. Based on our results and previous findings, a pathway of TBP degradation by *T. versicolor* is proposed in Fig. 3. Further investigation is still needed to elucidate the entire metabolic fate. On the other hand, *in silico* toxicity values for TBP and its proposed transformation products were determined using the Ecological Structure Activity Relationships (ECOSAR) Class Program (v2.2) (US Environmental Protection Agency, 2022). The predictions include acute toxicity values like the LC50 (lethal concentration for 50 % of the population) for fish and daphnia after 96 and 48 hours of exposure, respectively, and the EC50 (50 % effective concentration that causes a specific, non-lethal effect), for green algae growth inhibition after 96 hours of contact. These estimates are based on the molecular structure of each compound. The values were interpreted by comparing them to threshold values stablished by the Globally Harmonized System of Classification and Labelling of Chemicals (Winder et al., 2005). The compounds were categorized into four levels based on their LC50 and EC50 values: very toxic (< 1 mg/L), toxic (between 1 and 10 mg/L), harmful (between 10 and 100 mg/L) and not harmful (>100 mg/L). This toxicity analysis is depicted in Table S3. All transformation products exhibited lower toxicity than TBP for the three reported organisms, suggesting that the fungal treatment may contribute to detoxification.

### *3.4. Tributyl phosphate removal performance in TBR under non-sterile condition*

The trickle bed reactor constructed through immobilization has been proved as favorable system for fungal candidate to treat

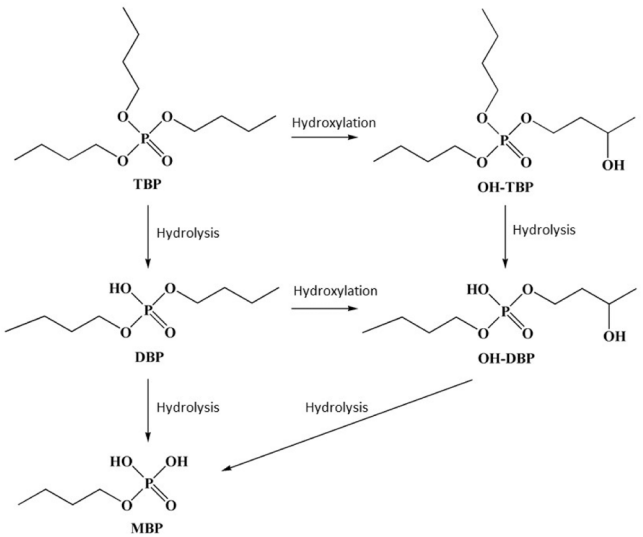


**Fig. 3.** Proposed pathway of TBP degradation by *T. versicolor*.

agricultural wastewater (Hu et al., 2021). Thus, it was employed for dealing with TBP contaminated water. As it is shown in Fig. 4, a considerable portion of the spiked pollutant was removed in the experimental reactor, yielding 93.4 % on average. It could be dominantly attributed to adsorption on wood chips since TBP removal maintained more than 93 % in abiotic reactor throughout 30 days-operation period. Indeed, the adsorption by lignocellulosic carrier seems to govern the removal of pollutant with high hydrophobicity, in wastewater treatment using this configuration (Hu et al., 2022, 2021). Besides, due to the limited contact time between immobilized fungus and pollutant (Hu et al., 2021), the involvement of CYP40 in TBP biodegradation was weakened. It can be also concluded that the biofilm negatively affected adsorption because lower removal (averagely 88.9 %) was obtained from heat-killed bed than abiotic control (96.7 % on average). Analogous to the experimental reactor, an observable decline in elimination efficiency towards TBP was exhibited in the heat-killed reactor, which might be the consequence of continuous elution.

Results from TBP monitoring in liquid phase at the end of each cycle suggested that adsorption made an important contribution to removal. Nevertheless, residues analysis towards solid phase evidenced that a degree of degradation occurred in three bioreactors (Table 2). In the experimental TBR where wood chips were initially colonized by *T. versicolor*, the concentration of pollutant on the wood was the lowest and global degradation percentage was 86.1 %. But this was very similar to the abiotic control (85.9 %), in which higher TBP residues were detected on the wood whereas the least amount was found in liquid phase. Those results noticed that a biological community harboring TBP degradation capacity was developed in the non-inoculated control reactor. On the contrary, in the killed control TBR, the amount of pollutant was higher in both phases. So, the heat-inactivated fungal film reduced the adsorption effect and also impeded the development of TBP degraders, yielding the lowest global degradation (63.7 %). Consequently, the identification of the microbial assemblage in the wood chips is very important to understand reactors' behavior.

Chemical oxygen demand (COD) and turbidity of the treated water were also monitored after each batch. A stepwise decrease in COD was demonstrated from the 1st round to 9th round in all sets. Then, a sudden rise was captured in the experimental reactor and heat-killed rector on the 10th batch (Table S4). The reasonable explanation could be either the release of wood particles due to fungal cell autolysis or the wood rotting by *T. versicolor*, and the later might also address the difference between experimental reactor and heat-killed reactor. Such behaviors also reflected in turbidity profile, showing as the $A_{650}$ of water eluted from the experimental reactor went down first and then went up (Table S4).

### 3.5. Microbial assemblage immobilized on wood chips

DGGE band profiles and UPGMA clustering analysis of the fungal communities in samples are presented in supplementary material Figure S1. DGGE fingerprints exhibited between 3 and 14 detectable bands of variable intensity. With reference to clustering analysis, two first-degree clusters were observed (60 % dissimilarity). The initially colonized wood (CW) was clearly separated from the experimental treatment, abiotic and killed controls, since the genetic profiles of the three replicates were consistent and very different compared to the rest of samples. Furthermore, profiles from abiotic control were clearly different (33 % dissimilarity) from killed control and experimental reactor, and in turn these two latter presented a similarity of 75.5 %.

46 bands were recovered from the gel and sequenced to determine their phylogenetic affiliation. Besides, the relative abundance of the dominant fungal populations was assessed. The position of these bands can be observed in Figure S1. Moreover, their similarity values compared to the most closely related GenBank sequences, and their phylogenetic affiliations are shown in Table S5. Overall, these sequences fell into two different phyla (Basidiomycota and Ascomycota), seven classes, and ten orders (Table S5). First and as expected, Basidiomycota represented 100 % of the colonized wood samples, since wood chips were only inoculated with *Trametes versicolor*, a member of this division. On the other hand, in the abiotic and killed controls as well as the experimental set from both

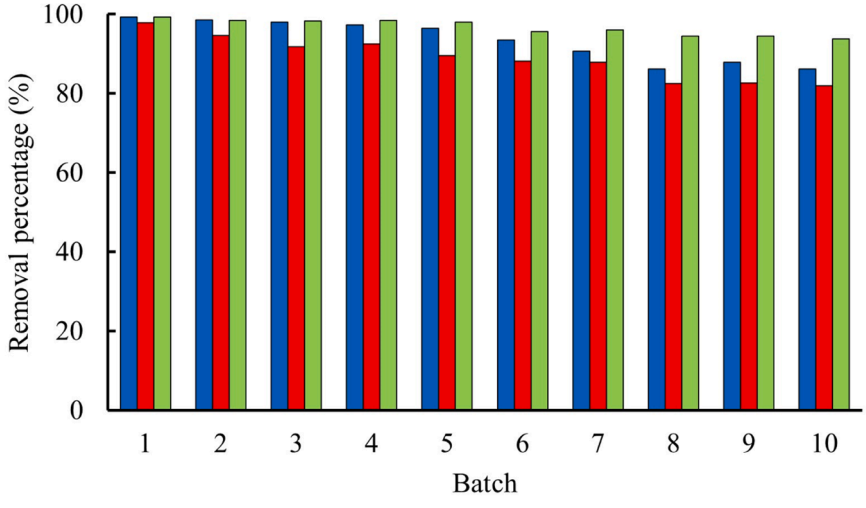


**Fig. 4.** Profile of TBP removal during by trickle bed reactors in sequencing batch mode under non-sterile condition. *Blue columns*, experimental reactor; *red columns*, heat-killed control; *green columns*, abiotic control.

**Table 2**
TBP mass balance in the TBR operating in 3-days SBR after 10 cycles.

| TBR | Mass of TBP (mg) | | | | Degradation (%) |
|---|---|---|---|---|---|
| | Initial | | Final | | |
| | Liquid phase | Solid phase | Liquid phase | Solid phase | |
| Experimental | 100 | 0 | 5.13 | 8.77 | 86.10 |
| Killed control | 100 | 0 | 7.78 | 28.5 | 63.72 |
| Abiotic control | 100 | 0 | 2.43 | 11.7 | 85.87 |

phyla were detected, but members from Basidiomycota were predominant.

Fungal relative abundance, expressed at the genus level, is shown in Fig. 5A. As was awaited, *T. versicolor* was the only fungus (100 %) that existed in colonized woodchips from both experimental reactor and killed control, before running period. After 30-day operation, the abundance of *T. versicolor* in the former dropped to 3.29 %, while it was not detected in the latter where *Apiotrichum*, an oleaginous yeast that has shown potential in the bioremediation of non-steroidal anti-inflammatory drugs (Peng et al., 2024), emerged as the predominant fungal phylotype (65.81 %). By contrast, *T. versicolor* in the experimental bioreactor was largely replaced by several fungal populations, among which also highlighted the genus *Apiotrichum* that constituted the most abundant phylotype and represented 55.99 % of the total fungal population abundance. Small amounts of the genus *Tremella* (5.51 %), which is known to be a parasite of other fungi, were also found in the experimental treatment. Finally, in the abiotic control, the most predominant fungal population corresponded to the genus *Naganishia* (68.33 %), which also belongs to the group of yeasts. These findings suggest that yeasts could be more competitive under these conditions. Direct evidence for the ecological processes mediating succession or causing ecological dominance remains scarce, but different dispersal abilities among species may be a key mechanism (Boynton et al., 2019). With reference to Richness, Shannon's diversity, and Pielou's evenness indexes presented in Fig. 5A. It can be observed that experimental treatment (EX) and killed control (KC) showed the highest values when compared with those of abiotic control (AC) and initial wood sample (CW). These results suggest that the presence of attached biomass on packed woodchips plays a determining role in the succession of microbial populations and then in the final composition of the fungal biomass regardless of whether the biomass is dead or alive.

The bacterial DGGE and the corresponding clustering analysis can be found in Figure S2. In this case, the number of bands ranged from 7 to 13, revealing small differences between experimental reactor and controls, as well as in comparison with the initially colonized wood samples. 37 bands were recovered and sequenced from the gel, and only one of them was discarded due to its ambiguous chimerical nature. Figure S2 also shows band positions, and their phylogenic affiliations are summarized in Table S6. The bacterial phylotypes belonged to three different phyla (Proteobacteria, Acidobacteria and Actinobacteria), which in turn were distributed into five classes and nine orders. In the initially colonized wood only members of six orders of the phylum Proteobacteria were detected. However, after 30-day operation, phylotypes belonging to seven different orders were detected in killed control, among which five corresponded to Proteobacteria, one to Acidobacteria and one to Actinobacteria. In the scenario of abiotic control, only members of the phylum Proteobacteria, belonging to six different orders, were found. Regarding experimental reactor, five different orders were detected; four of them included within the phylum Proteobacteria and the fifth belonging to Actinobacteria. About bacterial diversity shifts, the initial bacterial composition from initially colonized wood chips persisted in experimental reactor over time. By contrast, bacterial composition in both controls was very different from the previous ones, and they somehow shared many similarities that seemed to be related to the influent wastewater.

As for relative abundance, the most predominant genus from initially colonized wood samples was *Paraburkholderia* (64.8 %) (Fig. 5B), which is ubiquitously distributed in soils and is also found in decaying wood colonized by fungi (Christofides et al., 2020). This genus was also present in the experimental treatment (15.6 %) and in both abiotic and killed controls (19.4 % in KC and 0.7 % in AC), showing an association with the presence of *T. versicolor*. Different authors have revealed the potential of *Paraburkoholderia* in bioremediation as well as in promoting growth of fungal mycelia (Dias et al., 2019; Napitupulu et al., 2022), suggesting that could have a relevant role in the bioreactor microbial assemblage. Another genus that can be highlighted is *Curtobacterium* (6.10 % in EX and 2.91 % in KC), since it presents chitinolytic activity (Dimkić et al., 2021) and consequently can contribute to the detachment of fungal biomass from the wood matrix. In fact, it is only present in samples from EX and KC. On the other hand, members of the genus *Rhizobium* were also present, mainly in the abiotic and killed controls (27.49 % and 17.39 %, respectively). This genus has been evinced as degrader towards halogenated compounds similar to TBP (Bhandari et al., 2021) and Tris (2-chloroethyl) phosphate (TCEP) (Liang et al., 2022). *Novosphingobium* that possesses phosphatase enzymes that are related to OPFRs biodegradation (Yu et al., 2022) is also present in AC and KC. According to the mass balance (Table 2), the elimination of TBP in both controls was almost due to biodegradation, which can be most likely linked to *Rhizobium* and *Novosphingobium*. Furthermore, the former was also present in the experimental set and could contribute to TBP removal. It is well known that mixed microbial communities, including fungi and bacteria, with reach metabolic networks, interact with each other in the natural environment and can cooperate for the acquisition of nutrients (Deveau et al., 2018) and exhibit diverse synergistic mechanisms which plays a crucial role in enhancing the degradation of contaminants (Gu et al., 2022; Thirumalaivasan et al., 2024). Regarding R, H and E bacterial diversity indexes (Fig. 5B), the lowest mean values corresponded to colonized wood (CW), while the highest, as well as in the fungal populations, belonged to the killed control (KC) and experimental reactor (EX), and, revealing the importance of the immobilized biomass on microbial diversity.

Unsurprisingly, qPCR results showed that *Trametes versicolor* was only detected in the initial colonized wood sample and

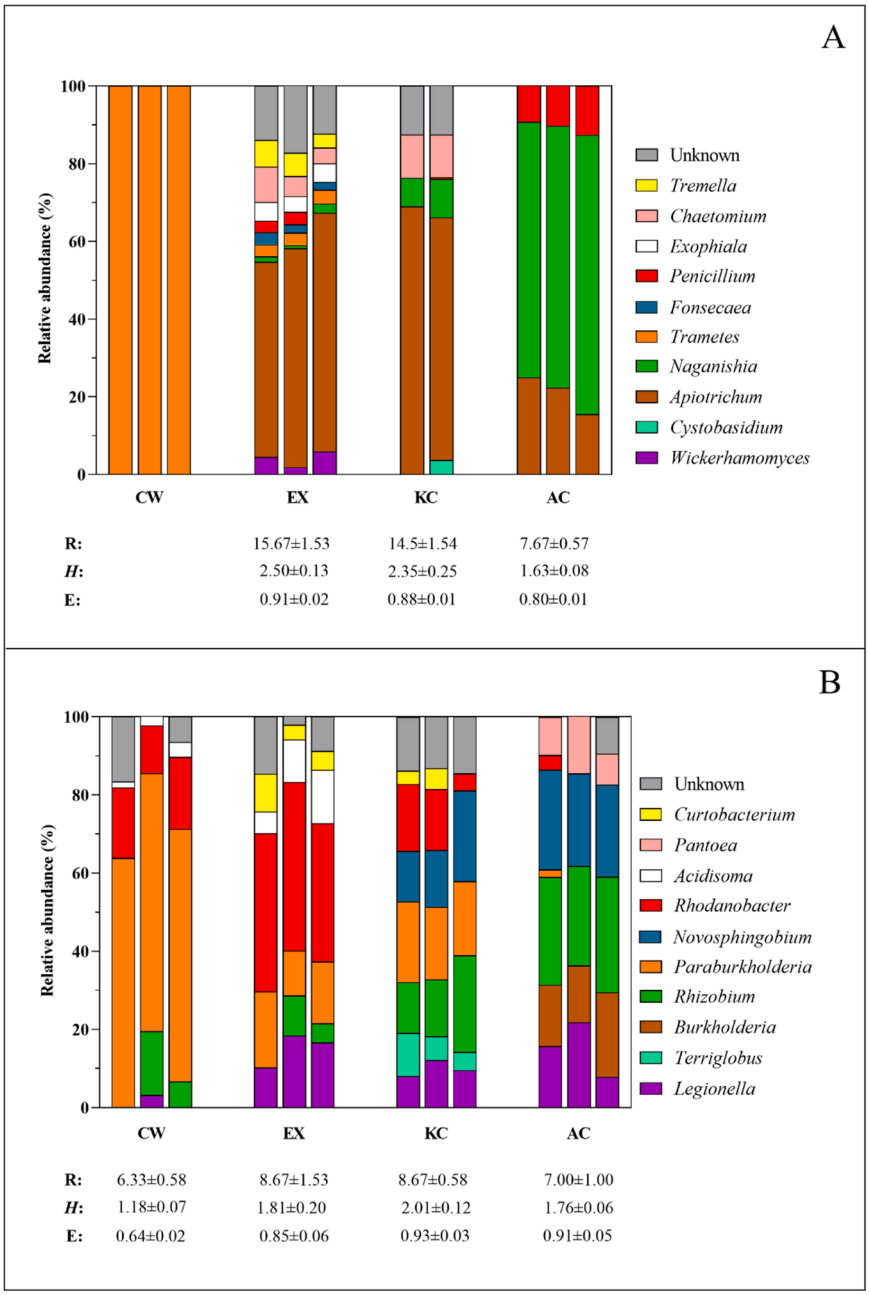


**Fig. 5.** Relative abundance of the fungal (A) and bacterial (B) taxonomical groups at the genus level in the immobilized biomass from the wood chips packed in the trickle bed reactor corresponding to abiotic control (AC), killed control (KC) and experimental treatment (EX), in comparison with initial colonized wood (CW) (left column); Three replicates are represented for each condition. Below each sample Shannon diversity index (*H*) Pielou's evenness index (E) and Richness (R) are indicated.

experimental reactor after running period (Fig. 6), however, it dropped significantly from 3,95E+08–8,09E+05 DNA copies/g of wood (Kolmogorov-Smirnov test p value=0.0001) (Table S7). Such decline was in accordance with the results obtained through the DGGE analysis that *T. versicolor* was largely replaced by other fungal populations such as *Apiotrichum*. With reference to total fungal population abundances, small variations were observed among all samples (Fig. 6). The experimental treatment exhibited the highest mean values, while it decreased significantly ($p < 0.05$) in abiotic control and initially colonized wood (Table S8). It is also worthy to mention that there was no significant difference between *Trametes versicolor* and total fungi abundances in initial wood sample (Table S7). In contrast, total bacterial abundance increased significantly after 30-day operating period, by two-orders of magnitude (Fig. 6), ascribed to non-sterile conditions. Besides, significantly lower ($p < 0.05$) total bacterial abundance was obtained from

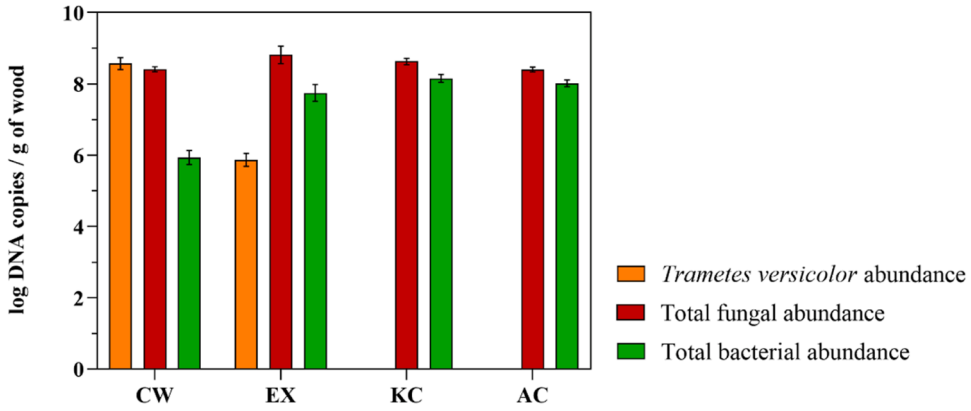


**Fig. 6.** Abundance of *Trametes versicolor* and total fungal and bacterial populations on the wood chips packed in the trickle bed reactor corresponding to abiotic control (AC), killed control (KC) and experimental treatment (EX) after 30-day operation, in comparison with initial colonized wood (CW), expressed as the log of DNA copies of the qPCR target amplicon by the dry mass of wood in grams.

experimental reactor compared with controls (Table S9), suggesting that the immobilization strategy was useful to control bacterial growth in fungal treatments, which keeps in line with the study of Hu et al. (Hu et al., 2022).

The microbial assemblage results showed that *Trametes versicolor* persisted throughout the 30-day operating period. Moreover, different bacterial populations have also been established on the cellulosic support packed into the trickled-bed bioreactors contributing to TBP clean up. This work has revealed that the WRF *T. versicolor* can efficiently carry out TBP biodegradation, but its combination with bacterial populations can contribute to enhance the process.

## 4. Conclusions

*Trametes versicolor* could efficiently remove tributyl phosphate, during which adsorption acted as the first step. The cytochrome P450 enzymatic system is involved in the degradation process while laccase is able to degrade TBP only with the presence of mediators. Up to four TPs were identified, which evidences that hydroxylation and hydrolysis played vital roles in TBP decomposition. The TBP removal by a tricked bed immobilized by *T. versicolor* on wood chips was also assayed, turned out that very high yield was obtained treating synthetic wastewater along 30-day running period in both experimental reactor and controls. In combination with global mass balance analysis, it can be assumed that degradation contributed largely to total removal. Further microbiota evolution analysis told that different bacterial populations had established on the lignocellulosic support besides *T. versicolor*, by which TBP degradation was enhanced. Future investigations should be addressed to the utilization of consortia for TBP removal and the evaluation of their environmental adaptability as well as stability.

## CRediT authorship contribution statement

**Soheila Shokrollahzadeh:** Writing – review & editing, Supervision. **Kaidi Hu:** Writing – review & editing, Formal analysis. **Núria Gaju:** Writing – review & editing, Supervision. **Montserrat Sarrà:** Funding acquisition, Conceptualization. **Maira Martínez-Alonso:** Supervision, Conceptualization. **Diana Losantos:** Writing – review & editing, Investigation. **Shamim Tayar:** Writing – original draft, Investigation. **Javier Villagra:** Investigation, Formal analysis.

## Declaration of Competing Interest

The authors declare that they have no known competing financial interests or personal relationships that could have appeared to influence the work reported in this paper.

## Acknowledgements

Projects: PID2019–103989RB-100 and PID2022–138929OB-I00 financed by MCIN/ AEI /10.13039/501100011033. This work has been partially supported by the Generalitat de Catalunya (Consolidated Research Group 2021-SGR-01008). Javier Villagra acknowledges PIF-UAB predoctoral grant B22P0008.

## Appendix A. Supporting information

Supplementary data associated with this article can be found in the online version at doi:10.1016/j.eti.2024.103867.

## Data Availability

Data will be made available on request.

## References


Arnold, L.L., Christenson, W.R., Cano, M., St John, M.K., Wahle, B.S., Cohen, S.M., 1997. Tributyl phosphate effects on urine and bladder epithelium in male sprague-dawley rats. FUNDAMENTAL Appl. Toxicol.

Auletta, C.S., Weiner, M.L., Richter, W.R., 1998. A dietary toxicity/oncogenicity study of tributyl phosphate in the rat 1. Toxicologist.

Bacaloni, A., Cavaliere, C., Foglia, P., Nazzari, M., Samperi, R., Laganà, A., 2007. Liquid chromatography/tandem mass spectrometry determination of organophosphorus flame retardants and plasticizers in drinking and surface waters. Rapid Commun. Mass Spectrom. 21, 1123–1130. https://doi.org/10.1002/rcm.2937.

Baiocco, P., Barreca, A.M., Fabbrini, M., Galli, C., Gentili, P., 2003. Promoting laccase activity towards non-phenolic substrates: A mechanistic investigation with some laccase-mediator systems. Org. Biomol. Chem. 1, 191–197. https://doi.org/10.1039/b208951c.

Beltrán-Flores, E., Tayar, S., Blánquez, P., Sarrà, M., 2023. Effect of dissolved oxygen on the degradation activity and consumption capacity of white-rot fungi. J. Water Process Eng. 55. https://doi.org/10.1016/j.jwpe.2023.104105.

Bhandari, S., Poudel, D.K., Marahatha, R., Dawadi, S., Khadayat, K., Phuyal, S., Shrestha, S., Gaire, S., Basnet, K., Khadka, U., Parajuli, N., 2021. Microbial Enzymes Used in Bioremediation. J. Chem. https://doi.org/10.1155/2021/8849512.

Blánquez, P., Casas, N., Font, X., Gabarrell, X., Sarrà, M., Caminal, G., Vicent, T., 2004. Mechanism of textile metal dye biotransformation by Trametes versicolor. Water Res 38, 2166–2172. https://doi.org/10.1016/j.watres.2004.01.019.

Boynton, P.J., Peterson, C.N., Pringle, A., 2019. Superior dispersal ability can lead to persistent ecological dominance throughout succession. Appl. Environ. Microbiol 85. https://doi.org/10.1128/AEM.02421-18.

Christofides, S.R., Bettridge, A., Farewell, D., Weightman, A.J., Boddy, L., 2020. The influence of migratory Paraburkholderia on growth and competition of wood-decay fungi. Fungal Ecol. 45, 100937. https://doi.org/10.1016/j.funeco.2020.100937.

Črešnar, B., Petrič, Š., 2011. Cytochrome P450 enzymes in the fungal kingdom. Biochim Biophys. Acta Proteins Prote. https://doi.org/10.1016/j.bbapap.2010.06.020.

Dang, Y., Tang, K., Wang, Z., Cui, H., Lei, J., Wang, D., Liu, N., Zhang, X., 2023. Organophosphate Esters (OPEs) Flame Retardants in Water: A Review of Photocatalysis, Adsorption, and Biological Degradation. Molecules. https://doi.org/10.3390/molecules28072983.

Deveau, A., Bonito, G., Uehling, J., Paoletti, M., Becker, M., Bindschedler, S., Hacquard, S., Hervé, V., Labbé, J., Lastovetsky, O.A., Mieszkin, S., Millet, L.J., Vajna, B., Junier, P., Bonfante, P., Krom, B.P., Olsson, S., van Elsas, J.D., Wick, L.Y., 2018. Bacterial–fungal interactions: ecology, mechanisms and challenges. FEMS Microbiol Rev. 42, 335–352. https://doi.org/10.1093/femsre/fuy008.

Dias, G.M., de Sousa Pires, A., Grilo, V.S., Castro, M.R., de Figueiredo Vilela, L., Neves, B.C., 2019. Comparative genomics of *Paraburkholderia kururiensis* and its potential in bioremediation, biofertilization, and biocontrol of plant pathogens. Microbiologyopen 8. https://doi.org/10.1002/mbo3.801.

Dimkić, I., Bhardwaj, V., Carpentieri-Pipolo, V., Kuzmanović, N., Degrassi, G., 2021. The chitinolytic activity of the Curtobacterium sp. isolated from field-grown soybean and analysis of its genome sequence. PLoS One 16, e0259465. https://doi.org/10.1371/journal.pone.0259465.

Dorn-In, S., Bassitta, R., Schwaiger, K., Bauer, J., Hölzel, C.S., 2015. Specific amplification of bacterial DNA by optimized so-called universal bacterial primers in samples rich of plant DNA. J. Microbiol Methods 113, 50–56. https://doi.org/10.1016/j.mimet.2015.04.001.

Eikenes, M., Hietala, A.M., Alfredsen, G., Gunnar Fossdal, C., Solheim, H., 2005. Comparison of quantitative real-time PCR, chitin and ergosterol assays for monitoring colonization of Trametes versicolor in birch wood. Holzforschung 59, 568–573. https://doi.org/10.1515/HF.2005.093.

Eltoukhy, A., Jia, Y., Lamraoui, I., Abo-Kadoum, M.A., Atta, O.M., Nahurira, R., Wang, J., Yan, Y., 2022. Transcriptome analysis and cytochrome P450 monooxygenase reveal the molecular mechanism of Bisphenol A degradation by Pseudomonas putida strain YC-AE1. BMC Microbiol 22, 294. https://doi.org/10.1186/s12866-022-02689-6.

Feickert Fenske, C., Kirzeder, F., Strübing, D., Koch, K., 2023. Biogas upgrading in a pilot-scale trickle bed reactor – Long-term biological methanation under real application conditions. Bioresour. Technol. 376, 128868. https://doi.org/10.1016/j.biortech.2023.128868.

García-Vara, M., Hu, K., Postigo, C., Olmo, L., Caminal, G., Sarrà, M., López de Alda, M., 2021. Remediation of bentazone contaminated water by Trametes versicolor: Characterization, identification of transformation products, and implementation in a trickle-bed reactor under non-sterile conditions. J. Hazard Mater. 409. https://doi.org/10.1016/j.jhazmat.2020.124476.

Gu, D., Xiang, X., Wu, Y., Zeng, J., Lin, X., 2022. Synergy between fungi and bacteria promotes polycyclic aromatic hydrocarbon cometabolism in lignin-amended soil. J. Hazard Mater. 425, 127958. https://doi.org/10.1016/j.jhazmat.2021.127958.

Hou, R., Lin, L., Li, H., Liu, S., Xu, X., Xu, Y., Jin, X., Yuan, Y., Wang, Z., 2021. Occurrence, bioaccumulation, fate, and risk assessment of novel brominated flame retardants (NBFRs) in aquatic environments — A critical review. Water Res. https://doi.org/10.1016/j.watres.2021.117168.

Hu, K., Torán, J., López-García, E., Barbieri, M.V., Postigo, C., de Alda, M.L., Caminal, G., Sarrà, M., Blánquez, P., 2020. Fungal bioremediation of diuron-contaminated waters: Evaluation of its degradation and the effect of amendable factors on its removal in a trickle-bed reactor under non-sterile conditions. Sci. Total Environ. 743. https://doi.org/10.1016/j.scitotenv.2020.140628.

Hu, K., Sarrà, M., Caminal, G., 2021. Comparison between two reactors using Trametes versicolor for agricultural wastewater treatment under non-sterile condition in sequencing batch mode. J. Environ. Manag. 293. https://doi.org/10.1016/j.jenvman.2021.112859.

Hu, K., Sarrà, M., Caminal, G., 2022. Oak wood provides suitable nutrients for long-term continuous pesticides removal by Trametes versicolor in a pilot plant trickle bed reactor. J. Clean. Prod. 380. https://doi.org/10.1016/j.jclepro.2022.135059.

Kim, J.W., Isobe, T., Chang, K.H., Amano, A., Maneja, R.H., Zamora, P.B., Siringan, F.P., Tanabe, S., 2011. Levels and distribution of organophosphorus flame retardants and plasticizers in fishes from Manila Bay, the Philippines. Environ. Pollut. 159, 3653–3659. https://doi.org/10.1016/j.envpol.2011.07.020.

Kirk, T.K., Schultz, E., Connors, W.J., Lorenz, L.F., Zeikus, J.G., 1978. Influence of Culture Parameters on Lignin Metabolism by Phanerochaete chrysosporium. Arch. Microbiol.

Kraft, V., Weber, W., Streipert, B., Wagner, R., Schultz, C., Winter, M., Nowak, S., 2015. Qualitative and quantitative investigation of organophosphates in an electrochemically and thermally treated lithium hexafluorophosphate-based lithium ion battery electrolyte by a developed liquid chromatography-tandem quadrupole mass spectrometry method. RSC Adv. 6, 8–17. https://doi.org/10.1039/c5ra23624j.

Kulkarni, S.V., Markad, V.L., Melo, J.S., D'Souza, S.F., Kodam, K.M., 2014. Biodegradation of tributyl phosphate using Klebsiella pneumoniae sp. S3. Appl. Microbiol Biotechnol. 98, 919–929. https://doi.org/10.1007/s00253-013-4938-2.

Liang, Y., Zhou, X., Wu, Yiding, Wu, Yang, Gao, S., Zeng, X., Yu, Z., 2022. Rhizobiales as the Key Member in the Synergistic Tris (2-chloroethyl) Phosphate (TCEP) Degradation by Two Bacterial Consortia. Water Res 218.

Liu, J., Lin, H., Dong, Y., Li, B., 2019. Elucidating the biodegradation mechanism of tributyl phosphate (TBP) by Sphingomonas sp. isolated from TBP-contaminated mine tailings. Environ. Pollut. 250, 284–291. https://doi.org/10.1016/j.envpol.2019.03.127.

Losantos, D., Sarra, M., Caminal, G., 2024. OPFR removal by white rot fungi: screening of removers and approach to the removal mechanism. Front. Fungal Biol. 5. https://doi.org/10.3389/ffunb.2024.1387541.

Lucas, D., Castellet-Rovira, F., Villagrasa, M., Badia-Fabregat, M., Barceló, D., Vicent, T., Caminal, G., Sarrà, M., Rodríguez-Mozaz, S., 2018. The role of sorption processes in the removal of pharmaceuticals by fungal treatment of wastewater. Sci. Total Environ. 610–611, 1147–1153. https://doi.org/10.1016/j.scitotenv.2017.08.118.

Marco-Urrea, E., Pérez-Trujillo, M., Vicent, T., Caminal, G., 2009. Ability of white-rot fungi to remove selected pharmaceuticals and identification of degradation products of ibuprofen by Trametes versicolor. Chemosphere 74, 765–772. https://doi.org/10.1016/j.chemosphere.2008.10.040.

Marklund, A., Andersson, B., Haglund, P., 2005. Organophosphorus flame retardants and plasticizers in Swedish sewage treatment plants. Environ. Sci. Technol. 39, 7423–7429. https://doi.org/10.1021/es051013l.
Martínez-Carballo, E., González-Barreiro, C., Sitka, A., Scharf, S., Gans, O., 2007. Determination of selected organophosphate esters in the aquatic environment of Austria. Sci. Total Environ. 388, 290–299. https://doi.org/10.1016/j.scitotenv.2007.08.005.
Maza-Márquez, P., Vílchez-Vargas, R., González-Martínez, A., González-López, J., Rodelas, B., 2018. Assessing the abundance of fungal populations in a full-scale membrane bioreactor (MBR) treating urban wastewater by using quantitative PCR (qPCR). J. Environ. Manag. 223, 1–8. https://doi.org/10.1016/j.jenvman.2018.05.093.
Meyer, J., Bester, K., 2004. Organophosphate flame retardants and plasticisers in wastewater treatment plants. J. Environ. Monit. 6, 599–605. https://doi.org/10.1039/b403206c.
Mir-Tutusaus, J.A., Masís-Mora, M., Corcellas, C., Eljarrat, E., Barceló, D., Sarrà, M., Caminal, G., Vicent, T., Rodríguez-Rodríguez, C.E., 2014. Degradation of selected agrochemicals by the white rot fungus Trametes versicolor. Sci. Total Environ. 500–501, 235–242. https://doi.org/10.1016/j.scitotenv.2014.08.116.
Mir-Tutusaus, J.A., Baccar, R., Caminal, G., Sarrà, M., 2018. Can white-rot fungi be a real wastewater treatment alternative for organic micropollutants removal? A review. Water Res. https://doi.org/10.1016/j.watres.2018.02.056.
Moussa, D., Brisset, J.L., 2003. Disposal of spent tributylphosphate by gliding arc plasma. J. Hazard Mater. 102, 189–200. https://doi.org/10.1016/S0304-3894(03)00069-4.
Nancharaiah, Y.V., Kiran Kumar Reddy, G., Krishna Mohan, T.V., Venugopalan, V.P., 2015. Biodegradation of tributyl phosphate, an organosphate triester, by aerobic granular biofilms. J. Hazard Mater. 283, 705–711. https://doi.org/10.1016/j.jhazmat.2014.09.065.
Napitupulu, T.P., Ayudhya, S.P.N., Aimi, T., Shimomura, N., 2022. Mycelial Growth-promoting Potential of Extracellular Metabolites of Paraburkholderia spp. Isolated from Rhizopogon roseolus Sporocarp. J. Pure Appl. Microbiol 16, 1154–1166. https://doi.org/10.22207/JPAM.16.2.43.
Peng, L., Yun, H., Ji, J., Zhang, W., Xu, T., Li, S., Wang, Z., Xie, L., Li, X., 2024. Biotransformation activities of fungal strain apiotrichum sp. IB-1 to ibuprofen and naproxen. Arch. Microbiol 206, 232. https://doi.org/10.1007/s00203-024-03963-z.
Pielou, E.C., 1966. The measurement of diversity in different types of biological collections. J. Theor. Biol. 13, 131–144. https://doi.org/10.1016/0022-5193(66)90013-0.
Pocostales, J.P., Sein, M.M., Knolle, W., Von Sonntag, C., Schmidt, T.C., 2010. Degradation of ozone-refractory organic phosphates in wastewater by ozone and ozone/hydrogen peroxide (peroxone): The role of ozone consumption by dissolved organic matter. Environ. Sci. Technol. 44, 8248–8253. https://doi.org/10.1021/es1018288.
Rangu, S.S., Singh, R., Gaur, N.K., Rath, D., Makde, R.D., Mukhopadhyaya, R., 2022. Isolation and characterization of a recombinant class C acid phosphatase from Sphingobium sp. RSMS strain. Biotechnol. Rep. 33, e00709. https://doi.org/10.1016/j.btre.2022.e00709.
Reemtsma, T., Quintana, J.B., Rodil, R., García-López, M., Rodríguez, I., 2008. Organophosphorus flame retardants and plasticizers in water and air I. Occurrence and fate. TrAC Trends Anal. Chem. 27, 727–737. https://doi.org/10.1016/j.trac.2008.07.002.
Rodil, R., Quintana, J.B., Concha-Graña, E., López-Mahía, P., Muniategui-Lorenzo, S., Prada-Rodríguez, D., 2012. Emerging pollutants in sewage, surface and drinking water in Galicia (NW Spain). Chemosphere 86, 1040–1049. https://doi.org/10.1016/j.chemosphere.2011.11.053.
Santín, G., Eljarrat, E., Barceló, D., 2016. Simultaneous determination of 16 organophosphorus flame retardants and plasticizers in fish by liquid chromatography-tandem mass spectrometry. J. Chromatogr. A 1441, 34–43. https://doi.org/10.1016/j.chroma.2016.02.058.
Shannon, C.E., 1984. A Mathematical Theory of Communication. Bell Syst. Tech. J.
Shi, Y., Gao, L., Li, W., Wang, Y., Liu, J., Cai, Y., 2016. Occurrence, distribution and seasonal variation of organophosphate flame retardants and plasticizers in urban surface water in Beijing, China. Environ. Pollut. 209, 1–10. https://doi.org/10.1016/j.envpol.2015.11.008.
Thirumalaivasan, N., Gnanasekaran, L., Kumar, S., Durvasulu, R., Sundaram, T., Rajendran, S., Nangan, S., Kanagaraj, K., 2024. Utilization of fungal and bacterial bioremediation techniques for the treatment of toxic waste and biowaste. Front Mater. 11. https://doi.org/10.3389/fmats.2024.1416445.
US Environmental Protection Agency, 2022. Ecological Structure Activity Relationships (ECOSAR) Predictive Model. [WWW Document]. URL ⟨https://www.epa.gov/tsca-screening-tools/ecological-structure-activity-relationships-ecosar-predictive-model⟩ (accessed 9.22.24).
Wariishi, H., Vallis, K., Gold, M.H., 1992. Manganese (II) oxidation by manganese peroxidase from the basidiomycete Phanerochaete chrysosporium. Kinetic mechanism and role of chelators. J. Biol. Chem. 267, 23689–23695.
Watts, M.J., Linden, K.G., 2008. Photooxidation and subsequent biodegradability of recalcitrant tri-alkyl phosphates TCEP and TBP in water. Water Res 42, 4949–4954. https://doi.org/10.1016/j.watres.2008.09.020.
Winder, C., Azzi, R., Wagner, D., 2005. The development of the globally harmonized system (GHS) of classification and labelling of hazardous chemicals. J. Hazard Mater. 125, 29–44. https://doi.org/10.1016/j.jhazmat.2005.05.035.
Wolschke, H., Sühring, R., Xie, Z., Ebinghaus, R., 2015. Organophosphorus flame retardants and plasticizers in the aquatic environment: A case study of the Elbe River, Germany. Environ. Pollut. 206, 488–493. https://doi.org/10.1016/j.envpol.2015.08.002.
World Health Organization, 1991. "Tri-n-Butyl Phosphate," Environmental Health Criteria.
Yang, X., Yu, G., Xu, L., Wang, J., 2022. Degradation of the mixed organic solvents of tributyl phosphate and n-dodecane by heterogeneous Fenton-like oxidation using nanoscale zero-valent iron as the catalyst. Chemosphere 292. https://doi.org/10.1016/j.chemosphere.2021.133449.
Yao, C., Li, Y., Jiang, C., Li, J., Jing, K., Zhang, S., Yang, H., Liu, C., Zhao, L., 2023. Triisobutyl phosphate biodegradation by enriched activated sludge consortia Degradation mechanism and bioaugmentation potential. Environ. Pollut. 322.
Yu, Y., Chen, J., Zhu, X., Yu, X., Zhou, H., Sun, J., Wang, Q., Yin, H., Zhu, L., 2022. New Insights into the Biodegradation of Organophosphorus Flame Retardants by Microbial Consortium: Mechanism, Risk and Application. SSRN Electron. J. https://doi.org/10.2139/ssrn.4042476.
Yuan, X., Lacorte, S., Cristale, J., Dantas, R.F., Sans, C., Esplugas, S., Qiang, Z., 2015. Removal of organophosphate esters from municipal secondary effluent by ozone and UV/H2O2 treatments. Sep Purif. Technol. 156, 1028–1034. https://doi.org/10.1016/j.seppur.2015.09.052.